

# EFFICIENT WPINN-APPROXIMATIONS TO ENTROPY SOLUTIONS OF HYPERBOLIC CONSERVATION LAWS

AIDAN CHAUMET AND JAN GIESSELMANN

**ABSTRACT.** We consider the approximation of weak solutions of nonlinear hyperbolic PDEs using neural networks, similar to the classical PINNs approach, but using a weak (dual) norm of the residual. This is a variant of what was termed “weak PINNs” recently. We provide some explicit computations that highlight why classical PINNs will not work well for discontinuous solutions to nonlinear hyperbolic conservation laws and we suggest some modifications to the weak PINN methodology that lead to more efficient computations and smaller errors.

## CONTENTS

1. Introduction	1
2. Basic Concepts and Definitions	4
2.1. Scalar Conservation Laws	4
2.2. Classical PINNs	5
2.3. Choice of Norm	6
2.4. A Variant of wPINNs — Motivation	11
2.5. Loss Definition	12
3. Algorithm and Implementation Details	13
3.1. Training Algorithm	14
3.2. Implementation Notes	14
4. Numerical Results	16
4.1. Comparison Setup	16
4.2. Standing Shock	17
4.3. Moving Shock	18
4.4. Rarefaction Wave	19
4.5. Sine Wave	20
5. Discussion	22
References	22

## 1. INTRODUCTION

Machine learning techniques and neural networks are extremely successful in a variety of applications ranging from computer vision to natural language processing. Mathematically, these tasks can be understood as function approximation. This success has triggered mathematical

---

*E-mail addresses:* chaumet@mathematik.tu-darmstadt.de, giesselmann@mathematik.tu-darmstadt.de.

*Date:* November 23, 2022.

*Key words and phrases.* physics-informed learning, PINNs, hyperbolic conservation laws, entropy solution.

studies into the use of neural networks in approximating solutions to partial differential equations.

Approaches for using machine learning to numerically approximate PDEs can be grouped into two classes, supervised and unsupervised learning. Supervised learning requires labeled data, which has to be created by observations or numerical schemes. There is vast literature on this topic. Some examples include [1–4]. The approach to be investigated in this paper is based on unsupervised learning. This approach is usually termed “Physics informed neural networks” (PINNs), based on the understanding that the PDE to be solved encodes our understanding of an underlying (physical) ground truth. Originally, PINNs go back to [5–7], but were popularized more recently in [2]. Interest in PINNs has grown rapidly since they offer versatile and efficient schemes, in particular for high-dimensional problems, one of the main benefits being their meshless nature. Some recent examples of these methods include [8], introducing the Deep Ritz Method, a PINN framework for elliptic problems, [9], presenting advancements in enforcing essential boundary conditions for the aforementioned framework, [10], wherein PINNs are applied to fractional advection-diffusion equations and [11], proposing a domain decomposition framework for PINNs for multiscale problems and to improve parallelization during training.

In their most frequently used form, PINNs are based on minimizing the  $L^2$  norm of the residual associated with the PDE, admitting interpretation of PINNs as a weighted least-squares point-collocation method [12, 13]. There has been tremendous progress in the convergence analysis of PINNs [14–16], that is based on three key principles [17]:

- (1) *Regularity* of the solutions to the underlying PDEs [...] which can be leveraged into proving that PDE residuals can be made arbitrarily small.
- (2) *Coercivity* (or stability) of the underlying PDEs, which ensures that the total error may be estimated in terms of residuals. For nonlinear PDEs, the constants in these coercivity estimates often depend on the regularity of the underlying solutions.
- (3) *Quadrature error* bounds for estimating the so-called generalization gap between the continuous and discrete versions of the PDE residual [18].

A key observation made in [17] is that for weak solutions of PDEs, because of their reduced regularity, it is usually not clear whether we can expect that good approximations in the space of neural functions, i.e. functions represented by neural networks, will lead to small residuals. More importantly, it is not clear whether minimizing residuals on the space of neural functions will lead to good approximations of the weak solution. Indeed there is numerical evidence that this is not the case [19]. As with point collocation methods, a key difficulty is that neural networks represent continuous functions, while weak solutions are generally not.

For point-collocation methods, it is crucial which norm is used for minimization, which extends to PINN-based methods as well. In [20], it is shown that for advection-reaction problems,  $L^2$  minimization of PDE residuals in general does not recover the unique viscosity solution to the problem. Instead, [21, 22] show that for linear first-order PDEs in one dimension, minimizing residuals with respect to the  $L^1$  norm in the space of piecewise linear functions for given boundary data is a fast and effective strategy that recovers the viscosity solution. The  $L^1$  minimization technique is then extended to (some) non-linear PDEs in one dimension, such as the Hamilton-Jacobi equations under the assumption that the exact solution is continuous and shown to be effective as well. However, [22] provides an example where  $L^1$  minimization fails to recover the correct viscosity solution for the inviscid Burgers equation for a discontinuous exact solution. An established strategy to approach this problem is by introducing artificial viscosity and solving the resulting regularized system [23].

These concepts can be applied to PINNs as well. For linear PDEs, training PINNs by minimizing the PDE residual in the  $L^1$  norm is effective because mollifying the exact solution produces a smooth approximation that solves an initial value problem with mollified initial data, which can readily be approximated using PINNs. Also, PINNs already approach problems with discontinuous solutions by viscous regularization [2], however this raises the question how much viscosity one needs to use to obtain solutions that can be learned effectively, yet are still “close” to the original solution.

There has been recent research into the choice of norm for training PINNs. In [24], it is suggested that for high-dimensional Hamilton-Jacobi-Bellmann equations, one should choose an  $L^p$ -based loss with sufficiently large  $p$ , and a procedure for training with respect to an  $L^\infty$ -based loss is outlined. Approximating solutions with reduced regularity has led to multiple variants of the PINN methodology, such as variational PINNs [25], the Deep Ritz Method [26] and weak PINNs [17]. The underlying idea of all these methods can be understood as minimizing the residual not in the  $L^2$  norm, but in some weak (dual) norm. While the Deep Ritz Method is specifically tailored to elliptic problems by using the fact that their solutions are minimizers of energy functionals, variational PINNs and weak PINNs address more general PDEs. Both of these methods measure the residual in a dual norm, but the key difference between the two is the way in which the test functions are represented. While variational PINNs use a mesh-based approach to represent test functions, weak PINNs represent the test functions by neural networks, thereby retaining the meshless nature of the method. The concept of weak PINNs was introduced on the prototypical example of scalar hyperbolic conservation laws in [17]. The authors provide a detailed convergence analysis as well as impressive numerical experiments, demonstrating the capability to approximate discontinuous solutions. Another approach to solving problems with discontinuous solutions is outlined in [27], where the residual is minimized in a weighted  $L^2$  norm with an adaptively chosen weight, chosen such that residuals close to steep gradients are weighted less.

Hyperbolic conservation laws arise in many models in continuum physics. Examples include the Euler and Shallow Water equations. The development of numerical schemes for hyperbolic conservation laws is quite mature, but there are new challenges that require schemes which are efficient in high space dimensions, e.g. the approximation of correlation measures that appear in the definition of statistical solutions [28]. One of the key challenges in dealing with hyperbolic conservation laws is that solutions are usually discontinuous and weak solutions are not unique.

The goal of this manuscript is twofold. Firstly, we will present some analytical computations that highlight mechanisms why minimizing  $L^1$ - or  $L^2$ - norms of residuals on the space of neural functions will not lead to good approximations of entropy solutions of nonlinear hyperbolic conservation laws and showcase the fundamental differences between the linear and nonlinear case. These arguments support that variational or weak PINNs are the appropriate framework when approximating nonlinear hyperbolic conservation laws.

Secondly, we propose some modifications to the original weak PINNs framework. The first modification is replacing the Kruzhkov entropy conditions by a single entropy condition. This is based on two considerations: Firstly, for systems of hyperbolic conservation laws there is usually only one physically motivated entropy. Secondly, for scalar hyperbolic conservation laws with convex flux function, enforcing any strictly convex entropy condition is equivalent to enforcing all Kruzhkov entropy conditions. The second modification relates to the computation of the dual norm. In the original weak PINNs methodology of [17], computing the dual norm involves a rather complicated maximization problem. We simplify this by identifying the maximizer as the solution of a family of elliptic problems which allows us to characterize it as the solution to

a concave maximization problem, similar to what is done in the Deep Ritz Method [26]. Our modified approach then consists of three networks, one representing the solution to the PDE and two networks responsible for computing dual norms of the PDE residual and an entropy residual, the latter measuring the violation of the entropy condition. To train these networks, one has to maximize the loss with respect to the two networks for computing the dual norms and minimize with respect to the network approximating the solution. Min-max problems of this type frequently arise in training (generative) adversarial networks [29, 30].

The outline of our paper is as follows. In Section 2 we give basic definitions for hyperbolic conservation laws and neural networks and provide computations that indicate why minimizing the  $L^2$  norm of the residual will not lead to good approximations of the weak solutions of hyperbolic conservation laws. In Section 3, we detail the implementation of our modified weak PINN algorithm and useful heuristics to accelerate training. In Section 4, we provide numerical experiments, showing that our variant of the weak PINN methodology leads to precise approximations of weak solutions of hyperbolic conservation laws for a variety of examples, while showing that the amount of training required to obtain good approximations is considerably smaller than in the original variant of weak PINNs. It will turn out that for simpler examples, the original weak PINNs and our variant give nearly identical results, while our variant outperforms the original version in the more challenging tests. We provide our implementation of the modified weak PINN algorithm under <https://git-ce.rwth-aachen.de/aidan.chaumet/wpinn>.

## 2. BASIC CONCEPTS AND DEFINITIONS

In this section we detail the problem setup and construction of a loss functional for weak entropy solutions to hyperbolic conservation laws. For simplicity, we discuss scalar conservation laws in one space dimension only. However, it is simple to extend general weak PINNs (wPINNs) and our modified approach to efficiently compute and train the loss functional to both systems endowed with a convex entropy and higher dimensions without additional conceptual hurdles.

**2.1. Scalar Conservation Laws.** We begin by recalling some basic facts about scalar conservation laws. We consider the scalar conservation law given by

$$\begin{cases} u_t + f(u)_x = 0 & \text{in } [0, T) \times \mathbb{R}, \\ u(0, \cdot) = u_0 & \text{on } \mathbb{R}, \end{cases} \quad (1)$$

where  $u$  is the *conserved quantity* and  $f \in C^2(\mathbb{R})$  is the *flux function*.

Oftentimes one wishes to work not on all of  $[0, T) \times \mathbb{R}$ , but rather restrict oneself to a compact interval  $D \subset \mathbb{R}$  in space. In this case one must supply boundary conditions, which need to be understood in a suitable weak sense, see [31, 32] and references therein. However, for initial conditions that are constant everywhere except on some compact interval in space, one knows that waves propagate with some maximum speed, such that the solution is constant outside some trapezoidal region in space-time. We limit our discussion to Dirichlet boundary conditions on space intervals  $D$  such that the left- and right boundary are outside of this trapezoid for the given time interval  $[0, T)$ . We denote the boundary conditions by  $u(t, x) = g(t, x)$  for  $(t, x) \in (0, T) \times \partial D$ . How to extend wPINNs to more complicated boundary conditions is an important question, but beyond the scope of this work.

Even for very simple flux functions and smooth initial conditions, one may obtain discontinuous solutions after finite time. Hence, one has to work with weak solutions:

**Definition 1** (Weak Solution). We call  $u \in L^\infty([0, T] \times \mathbb{R})$  a weak solution of problem (1)-(2) for some initial datum  $u_0 \in L^\infty(\mathbb{R})$ , if it satisfies

$$\int_{[0, T]} \int_{\mathbb{R}} u \varphi_t + f(u) \varphi_x \, dx \, dt + \int_{\mathbb{R}} u_0 \varphi(0, \cdot) \, dx = 0, \quad (3)$$

for any test function  $\varphi \in C_c^1([0, T] \times \mathbb{R})$ .

Weak solutions are, in general, not unique. One strategy to establish uniqueness is by imposing *entropy admissibility conditions* on weak solutions [33]. We define entropies  $\eta$  and corresponding entropy fluxes  $q$  as follows.

**Definition 2** (Entropy – Entropy Flux Pair). Let  $f \in W_{\text{loc}}^{1, \infty}(\mathbb{R}; \mathbb{R})$ . Then, for  $\eta, q \in W_{\text{loc}}^{1, \infty}(\mathbb{R}; \mathbb{R})$  we say that  $(\eta, q)$  are a *convex entropy-entropy flux pair*, if  $\eta$  is strictly convex and  $q' = f'\eta'$  almost everywhere.

Using the notion of entropy-entropy flux pairs one may define *entropy-admissible* solutions to problem (1)-(2).

**Definition 3** (Entropy Admissibility). We call  $u$  an *entropy-admissible* solution to the Cauchy problem (1)-(2) if it is a weak solution in the sense of Definition 1 and for any convex entropy-entropy flux pair, it satisfies

$$\eta(u)_t + q(u)_x \leq 0 \quad \text{in } [0, T] \times \mathbb{R} \quad (4)$$

in a distributional sense.

If the flux function  $f$  is strictly convex, then a weak solution  $u$  satisfying equation (4) for a single strictly convex entropy-entropy flux pair is entropy-admissible [34, 35]. Further, entropy-admissible solutions are unique. In the following we will assume that we are always working with fluxes  $f$  as above.

**2.2. Classical PINNs.** In the following, we discuss different solution strategies for neural network-based PDE solvers on the example of fully connected feed-forward neural networks with hidden layers of uniform width to approximate solutions to scalar conservation laws. Note that there are a multitude of more complicated network architectures, as studied in other works, e.g. [8, 26]. Mathematically we define such neural networks as follows:

**Definition 4** (Fully Connected NN). Let  $l, w \in \mathbb{N}$ . Let  $d \in \mathbb{N}$  be the input dimension. Let  $\sigma : \mathbb{R} \rightarrow \mathbb{R}$  be a smooth, non-linear function. We call  $\sigma$  the *activation function*.

Set  $L^{[0]}(x) := W^{[0]}x + b^{[0]}$  with  $W^{[0]} \in \mathbb{R}^{w \times d}$  and  $b^{[0]} \in \mathbb{R}^w$ . Further, set  $L^{[i]}(x) := W^{[i]}x + b^{[i]}$  with  $W^{[i]} \in \mathbb{R}^{w \times w}$  and  $b^{[i]} \in \mathbb{R}^w$  for  $i = 1, \dots, l-1$ . Finally, set  $L^{[l]}(x) := W^{[l]}x + b^{[l]}$  with  $W^{[l]} \in \mathbb{R}^{1 \times w}$  and  $b^{[l]} \in \mathbb{R}$ . We call the matrices  $W^{[i]}, i = 0, \dots, l$  the *weights* and  $b^{[i]}$  the *biases* of a neural network. The affine linear maps  $L^{[i]}$  are called the *layers* of the neural network. We say that the network has  $l$  layers with width  $w$ , where layers  $1, \dots, l-1$  are called *hidden layers*.

The set of weights and biases are called the *parameters* of the neural network, given by  $\theta := \{W^{[i]}, b^{[i]}\}_{i=0, \dots, l}$ .

Then, the *neural network* associated with the parameters  $\theta$  is a map  $u_\theta \in C^\infty(\mathbb{R}^d, \mathbb{R})$  given by

$$u_\theta = L^{[l]} \circ \sigma \circ L^{[l-1]} \circ \sigma \dots \circ \sigma \circ L^{[1]} \circ \sigma \circ L^{[0]}, \quad (5)$$

where we understand the composition with  $\sigma$  to mean the element-wise application to the layer output.

**Remark 1.** *Definition 4 refers to a very simple type of neural network. Clearly, one may allow different layers to have different widths, choose different activations for each layer or allow more complicated operations involving the layer output than just composition, say addition of previous layer outputs, for example in ResNets [36]. We limit our analysis to this type of network to focus on the effect of the choice of loss function, however our arguments extend to different architectures as well.*

*For the scope of this work, we limit ourselves to smooth activation functions by definition. It should be noted that a popular choice of activation is the  $\text{ReLU}(\cdot) := \max(0, \cdot)$  function, which is not smooth. Our analysis applies to ReLU networks as well, however in our numerical experiments this choice of activation function performed worse than smooth alternatives.*

PINN-based methods aim to minimize the PDE residuals measured in some discrete approximation of some function norm. Additional loss contributions may be used to weakly impose initial- and boundary conditions. Alternatively, initial- and boundary conditions can be encoded into the network design exactly. For  $v \in C^1([0, T] \times D)$ , we define the pointwise PDE residual as

$$\mathcal{R}[v] := v_t + f(v)_x \in C^0([0, T] \times D). \quad (6)$$

Let  $u_\theta$  be a neural network for parameters  $\theta$ , then the classical PINN approach defines the interior contribution to the neural network loss function as a Monte-Carlo approximation of the  $L^2$ -in-space-time norm of  $\mathcal{R}[u_\theta]$ . This is done by randomly choosing *collocation points*  $\{t_i, x_i\}_{i=1}^{N_c}$  with  $t_i \in [0, T]$ ,  $x_i \in D$  and  $N_c$  the number of collocation points, and then computing

$$\mathfrak{L}_{\text{int}}(u_\theta) := \frac{1}{N_c} \sum_{i=1}^{N_c} |\mathcal{R}[u_\theta](t_i, x_i)|^2. \quad (7)$$

Likewise, by sampling points in the domain  $D$  at  $t = 0$  one introduces the initial condition into the overall loss. Similarly, for the boundary condition  $u = g$  on  $(0, T) \times \partial D$ , we get a boundary contribution to the overall loss as

$$\mathfrak{L}_{\text{ic}}(u_\theta) = \|u_\theta(0, \cdot) - u_0\|_{2, \text{MC}} \quad \text{and} \quad \mathfrak{L}_{\text{bc}}(u_\theta) = \|u_\theta - g\|_{2, \text{MC}}, \quad (8)$$

where  $\|\cdot\|_{2, \text{MC}}$  denotes a Monte-Carlo approximation to the  $L^2$ -norm on the respective sets. The overall loss is then the weighted sum of interior, initial and boundary loss,  $\mathfrak{L}(u_\theta) := \mathfrak{L}_{\text{int}} + \lambda(\mathfrak{L}_{\text{ic}} + \mathfrak{L}_{\text{bc}})$  with some user-chosen hyperparameter  $\lambda$  setting the relative importance of the two terms [37]. As empirically observed in [3], this approach based on minimizing the  $L^2$  norm of the interior residual does not work for learning discontinuous solutions to hyperbolic conservation laws.

**2.3. Choice of Norm.** In the following, we present an illustrative argument that reasons why the classical PINN approach cannot learn the correct solution based on the example of standing shock solutions to the inviscid Burgers equation. However, we note that the intuition we develop here easily extends to other nonlinear hyperbolic conservation laws and moving shocks.

Consider that by construction, for continuous activation functions  $\sigma$ , neural networks are continuous as well, such that it is impossible to represent discontinuities exactly. As such, one expects a reasonable neural network approximation to a discontinuous solution to learn a smoothed-out version of the underlying shock, such that it will be “close” to the underlying solution in a pointwise sense outside of a small region around discontinuities and in an  $L^2$ -sense for the entire domain.

As a concrete example we consider the inviscid Burgers equation, that is the scalar conservation law for the flux function  $f(u) = \frac{1}{2}u^2$  and the initial condition

$$u_0(x) = \begin{cases} 1 & \text{for } x < 0, \\ -1 & \text{for } x \geq 0, \end{cases} \quad (9)$$

having a standing shock as the true solution.

As a first scenario we consider time-independent approximations to the solution of this problem, as the underlying solution is time-independent as well and this avoids complications caused by time-dependent approximations. We consider “reasonable” approximate solutions  $\tilde{u}$  which are smooth and satisfy

$$\begin{cases} \tilde{u}(x) \in [1 - \epsilon, 1 + \epsilon] & \text{for } x < -\epsilon, \\ \tilde{u}(x) \in [-1 - \epsilon, -1 + \epsilon] & \text{for } x > \epsilon, \\ \tilde{u}(x) \in [-1 - \epsilon, 1 + \epsilon] & \text{for } -\epsilon \leq x \leq \epsilon \end{cases} \quad (10)$$

for some  $\epsilon > 0$ . For  $\epsilon \rightarrow 0$  one easily checks that such approximations converge towards the exact solution in  $L^2([0, T] \times D)$  with a rate of  $\sqrt{\epsilon}$ . Our key argument now is that these reasonable approximations will, in fact, not produce a small  $L^2$  norm of the PDE residual, such that a PINN would not learn such approximations during the optimization process. We show that the  $L^2$  norm of the residual scales as  $\frac{1}{\sqrt{\epsilon}}$  in this case.

We begin by noting that it suffices to consider only the contribution to the residual from  $[0, T] \times (-\epsilon, \epsilon)$ , as the shock front is what contributes to the residual growing large and

$$\|\mathcal{R}[\tilde{u}]\|_{L^2([0, T] \times D)} \geq \|\mathcal{R}[\tilde{u}]\|_{L^2([0, T] \times (-\epsilon, \epsilon))}.$$

Outside of this region, approximating the true solution is easy and there exist good approximations with small residuals.

Then, from Hölder’s inequality it follows that  $\|\mathcal{R}[\tilde{u}]\|_{L^1([0, T] \times (-\epsilon, \epsilon))} \leq \sqrt{2\epsilon T} \|\mathcal{R}[\tilde{u}]\|_{L^2([0, T] \times (-\epsilon, \epsilon))}$ . As a second preliminary observation we note that for small enough  $\epsilon$ , because  $\tilde{u}(-\epsilon) > 0$  and  $\tilde{u}(\epsilon) < 0$  and  $\tilde{u}$  is continuous, there is at least one zero  $\bar{x}$  of  $\tilde{u}$  in  $(-\epsilon, \epsilon)$ . Hence, we also have  $f(\tilde{u}(\bar{x})) = 0$ . This behavior around the discontinuity is what makes the residual large, because contrary to the true solution which has a flux of  $f(u) = \frac{1}{2}$  everywhere, there is a region where  $|f(\tilde{u})_x|$  is large. Then we compute:

$$\begin{aligned} \|\mathcal{R}[\tilde{u}]\|_{L^1([0, T] \times (-\epsilon, \epsilon))} &= \int_0^T \int_{-\epsilon}^{\epsilon} |f(\tilde{u})_x| dx dt \\ &\geq \int_0^T \int_{-\epsilon}^{\bar{x}} |f(\tilde{u})_x| dx dt + \int_{\bar{x}}^{\epsilon} |f(\tilde{u})_x| dx dt \\ &\geq \int_0^T \left| \int_{-\epsilon}^{\bar{x}} f(\tilde{u})_x dx \right| dt + \left| \int_{\bar{x}}^{\epsilon} f(\tilde{u})_x dx \right| dt \\ &= \int_0^T \frac{1}{2} \tilde{u}(-\epsilon)^2 + \frac{1}{2} \tilde{u}(\epsilon)^2 dt \geq T(1 - \epsilon)^2, \end{aligned} \quad (11)$$

where in the last line we inserted the flux function for the Burgers equation explicitly.

Alongside our preliminary considerations this gives the overall estimate for the  $L^2$  residual loss:

$$\|\mathcal{R}[\tilde{u}]\|_{L^2([0, T] \times D)} \geq \|\mathcal{R}[\tilde{u}]\|_{L^2([0, T] \times (-\epsilon, \epsilon))} \geq \frac{\|\mathcal{R}[\tilde{u}]\|_{L^1([0, T] \times (-\epsilon, \epsilon))}}{2\sqrt{\epsilon T}} \geq \frac{\sqrt{T}(1 - \epsilon)^2}{2\sqrt{\epsilon}}. \quad (12)$$

As this estimate shows, for time-independent reasonable approximations to shock solutions of the Burgers equation, reducing  $\epsilon$ , which intuitively makes the approximation better, increases the  $L^2$ -norm of its residual.

We are not able to prove a similar estimate for the general case of time-dependent approximations satisfying (10) for each  $t$ . However, we consider two examples of typical time dependence, which cover a wide range of possible approximations and show that these do not produce a small  $L^2$ -norm of the residual either.

As a second example we consider approximations whose solution profile is shifted with some time-dependent velocity, but whose shape does not change. This means we consider time-dependent approximations of the form  $\tilde{u}(x - s(t))$  with  $\tilde{u}$  as in (10) for a smooth function  $s$  denoting the overall shift of the solution. Then the time derivative of such approximations is given by  $\tilde{u}_t = -s'\tilde{u}_x$ . The velocity of the profile is given by  $v := s'$ . Analogous to the previous computation for the  $L^1$ -in-space-time norm we compute

$$\begin{aligned} \int_0^T \int_{-\epsilon+s}^{\epsilon+s} |f(\tilde{u})_x + \tilde{u}_t| dx dt &\geq \int_0^T \left| \int_{-\epsilon+s}^{\bar{x}+s} f(\tilde{u})_x - v\tilde{u}_x dx \right| dt + \int_0^T \left| \int_{\bar{x}+s}^{\epsilon+s} f(\tilde{u})_x - v\tilde{u}_x dx \right| dt \\ &= \int_0^T \left| \underbrace{f(\tilde{u}(-\epsilon)) - v(t)\tilde{u}(-\epsilon)}_{=:A} \right| + \left| \underbrace{f(\tilde{u}(\epsilon)) - v(t)\tilde{u}(\epsilon)}_{=:B} \right| dt \\ &\geq \frac{T}{2} (1 - \epsilon)^2 + (1 - \epsilon) \|v\|_{L^1([0,T])}. \end{aligned} \tag{13}$$

For the last inequality of above computation, we use that  $\tilde{u}(\epsilon)$  and  $\tilde{u}(-\epsilon)$  have opposing sign, such that regardless of the sign of  $v(t)$ , either  $A$  or  $B$  is the sum of two positive contributions, while the other has mixed sign. For the sum of two positive terms, we may leave out the absolute value and we drop the contribution from the mixed term. Then the same arguments as before show that the  $L^2$  norm grows as  $\frac{1}{\sqrt{\epsilon}}$  again.

Note that for linear PDEs, this argument does not hold because  $f(\tilde{u}(-\epsilon))$  and  $f(\tilde{u}(\epsilon))$  have different signs, so one does not obtain a lower bound, showing that the linear case is fundamentally different. In fact, for the linear case we expect  $L^1$  minimization to work well, similar to the results from [22] that outlines this technique for mesh-based functions. For linear advection with constant velocity, by choosing the correct time-dependent shift function, it is clear that the residual can be made to vanish exactly. The overall loss then consists only of the violation of initial- and boundary conditions. However, arbitrarily precise smooth approximations can be constructed for given discontinuous initial data using mollifiers. Neural networks can then easily learn approximations of this type that lead to small losses.

As a final illustrative example we consider another class of time-dependent approximate solutions  $\tilde{u}$  with

$$\begin{cases} \tilde{u}(t, x) \in [1 - \epsilon, 1 + \epsilon] & \text{for } x < -\epsilon, \\ \tilde{u}(t, x) \in [-1 - \epsilon, -1 + \epsilon] & \text{for } x \geq \epsilon, \\ \tilde{u}(t, x) \in [1 + \epsilon, -1 - \epsilon] & \text{for } -\epsilon \leq x \leq \epsilon \end{cases} \tag{14}$$

such that there exists an  $\bar{x}$ , independent of  $t$ , with  $\tilde{u}(t, \bar{x}) = 0$ . The existence of a  $\bar{x}(t)$  is analogous to previously, however the restriction to time-independent  $\bar{x}$  is technical in nature. Further, we assume that  $(\bar{x} - x)\tilde{u}(x) \geq 0$  for all  $x \in D$ . Then we may perform a similar



computation as before:

$$\begin{aligned}
\|\mathcal{R}[\tilde{u}]\|_{L^1([0,T] \times (-\epsilon, \epsilon))} &= \int_0^T \int_{-\epsilon}^{\epsilon} |f(\tilde{u})_x + \tilde{u}_t| dx dt \\
&\geq \int_0^T \left| \int_{-\epsilon}^{\bar{x}} f(\tilde{u})_x + \tilde{u}_t dx \right| dt + \left| \int_{\bar{x}}^{\epsilon} f(\tilde{u})_x + \tilde{u}_t dx \right| dt \\
&= \int_0^T \left| f(\tilde{u}(t, -\epsilon)) - \int_{-\epsilon}^{\bar{x}} \tilde{u}_t dx \right| + \left| f(\tilde{u}(t, \epsilon)) + \int_{\bar{x}}^{\epsilon} \tilde{u}_t dx \right| dt \\
&\geq \int_0^T \left( f(\tilde{u}(t, -\epsilon)) + \int_{-\epsilon}^{\bar{x}} (\tilde{u}_t)^\ominus dx - \int_{\bar{x}}^{\epsilon} (\tilde{u}_t)^\oplus dx \right. \\
&\quad \left. + f(\tilde{u}(t, \epsilon)) - \int_{\bar{x}}^{\epsilon} (\tilde{u}_t)^\ominus dx + \int_{\bar{x}}^{\epsilon} (\tilde{u}_t)^\oplus dx \right) dt.
\end{aligned} \tag{15}$$

where  $(\cdot)^\ominus$  and  $(\cdot)^\oplus$  denote the negative and positive part of a function respectively. Then, because  $\bar{x}$  is independent of  $t$ , we may swap the order of integration and use the fact that

$$\left| \int_0^T (\tilde{u}_t)^\oplus(t, x) - (\tilde{u}_t)^\ominus(t, x) dt \right| = \left| \int_0^T \tilde{u}_t(t, x) dt \right| = |\tilde{u}(T, x) - \tilde{u}(0, x)| \leq 1 + \epsilon. \tag{16}$$

Inserting this into the last line of (15) gives

$$\begin{aligned}
\|\mathcal{R}[\tilde{u}]\|_{L^1([0,T] \times (-\epsilon, \epsilon))} &\geq T(1 - \epsilon)^2 - \int_{-\epsilon}^{\bar{x}} 1 + \epsilon dx - \int_{\bar{x}}^{\epsilon} 1 + \epsilon dx \\
&\geq T(1 - \epsilon)^2 - 2\epsilon(1 + \epsilon),
\end{aligned} \tag{17}$$

and we may conclude our estimate analogously to equation (12), giving a lower bound scaling as  $\frac{1}{\sqrt{\epsilon}}$ .

We see that for fairly general reasonable approximations, in each case the  $L^2$ -in-space-time norm of the PDE residual grows large for small  $\epsilon$ , while the magnitude of the  $L^1$  norm does not seem to be connected to  $\epsilon$ . This shows that both these norms are unsuitable choices for the loss function of a PINN then, because training networks by minimizing the resulting loss functions will not learn approximations with small  $\epsilon$ .

Instead, we motivate that, as argued in [17], one should consider a weaker norm of the residual. We argue that using the  $L^2$ -in time  $H^{-1}$ -in space ( $L^2$ - $H^{-1}$ -norm for short) norm is a good choice for this setting. Consider again the toy problem as outlined in (9) with a smooth approximation  $\tilde{u}$  as in (10). For technical simplicity we will limit ourselves to approximations that are constant in time, that is  $\tilde{u}(t, x) = \tilde{u}(0, x)$  for all  $(t, x)$  in  $[0, T] \times D$ .

We show that the value of the residual of approximate solutions of the form (10) goes to zero for  $\epsilon \rightarrow 0$  provided that the sequence is sufficiently non-oscillatory, i.e. if  $\epsilon^{\frac{3}{2}} \|f(\tilde{u})_x\|_{L^\infty([0,T] \times (-\epsilon, \epsilon))}$  and  $\|f(\tilde{u})_x\|_{L^2([0,T] \times (D \setminus (-\epsilon, \epsilon)))}$  both go to zero, which is a desirable property of an approximation.

Let  $V := H_0^1(D)$  with  $\|\cdot\|_V := \|\cdot\|_{H^1}$ , and let  $S := \{\varphi \in V : \|\varphi\|_V = 1\}$ . Then by definition of the  $H^{-1}$  norm, we compute

$$\begin{aligned} \|\mathcal{R}[\tilde{u}]\|_{L^2([0,T];H^{-1}(D))}^2 &= \int_{[0,T)} \left( \sup_{\varphi \in S} \int_D f(\tilde{u})_x \varphi \, dx \right)^2 dt \\ &\leq \int_{[0,T)} \left( \sup_{\varphi \in S} \int_{(-\epsilon,\epsilon)} f(\tilde{u})_x \varphi \, dx \right)^2 dt + \int_{[0,T)} \left( \sup_{\varphi \in S} \int_{D \setminus (-\epsilon,\epsilon)} f(\tilde{u})_x \varphi \, dx \right)^2 dt \end{aligned} \quad (18)$$

To estimate the first term of (18), we rewrite  $\varphi(x) = \varphi(0) + \int_0^x \varphi'(s) \, ds$  and use the fact that  $|f(\tilde{u}(t, \epsilon)) - f(\tilde{u}(t, -\epsilon))| \leq 4\epsilon$  for the Burgers equation under previous assumptions on  $\tilde{u}$  to conclude that

$$\begin{aligned} \int_0^T \left( \sup_{\varphi \in S} \int_{-\epsilon}^{\epsilon} f(\tilde{u})_x \varphi \, dx \right)^2 dt &= \int_0^T \left( \sup_{\varphi \in S} \left( \varphi(0) (f(\tilde{u}(t, \epsilon)) - f(\tilde{u}(t, -\epsilon))) \right. \right. \\ &\quad \left. \left. + \int_{-\epsilon}^{\epsilon} f(\tilde{u})_x \int_0^x \varphi'(s) \, ds \, dx \right) \right)^2 dt \\ &\leq \int_0^T \left( \sup_{\varphi \in S} \|f(\tilde{u})_x\|_{\infty} \int_{-\epsilon}^{\epsilon} \int_0^x |\varphi'(s)| \, ds \, dx + 4\epsilon \varphi(0) \right)^2 dt \quad (19) \\ &\leq \int_0^T \left( \sup_{\varphi \in S} \|f(\tilde{u})_x\|_{\infty} \int_{-\epsilon}^{\epsilon} \sqrt{|x|} \|\varphi'\|_{L^2(D)} \, dx + 4\epsilon \varphi(0) \right)^2 dt \\ &= T \sup_{\varphi \in S} \left( \|f(\tilde{u})_x\|_{\infty} \left( 2\epsilon^{\frac{3}{2}} \right) \|\varphi'\|_{L^2(D)} + 4\epsilon \varphi(0) \right)^2 \\ &\leq T \left( \|f(\tilde{u})_x\|_{\infty} \left( 2\epsilon^{\frac{3}{2}} \right) + 4\epsilon c_S \right)^2. \end{aligned}$$

The last inequality uses that, by definition,  $\|\varphi'\|_{L^2(D)} \leq 1$  and that in one dimension  $H^1$  is continuously embedded in  $L^\infty$  with embedding constant denoted by  $c_S$ .

Estimating the second term of (18) is straightforward. Note that by definition and applying Hölder's inequality, one sees that

$$\int_{[0,T)} \left( \sup_{\varphi \in S} \int_{D \setminus (-\epsilon,\epsilon)} f(\tilde{u})_x \varphi \, dx \right)^2 dt \leq \int_{[0,T)} \int_{D \setminus (-\epsilon,\epsilon)} f(\tilde{u})_x^2 \, dx \, dt = T \|f(\tilde{u})_x\|_{L^2([0,T) \times (D \setminus (-\epsilon,\epsilon)))}^2. \quad (20)$$

Combining the estimates for each of the two previous terms, we may estimate the residual in this norm by

$$\|\mathcal{R}[\tilde{u}]\|_{L^2([0,T);H^{-1}(D))}^2 \leq T \left( \left( \|f(\tilde{u})_x\|_{\infty} \left( 2\epsilon^{\frac{3}{2}} \right) + 4\epsilon c_S \right)^2 + \|f(\tilde{u})_x\|_{L^2([0,T) \times (D \setminus (-\epsilon,\epsilon)))}^2 \right). \quad (21)$$

This shows that the  $L^2$ - $H^{-1}$  norm is a good choice of norm for the PDE residual in the neural network loss function, because equation (21) shows that a small loss corresponds to a good approximation of the underlying solution. Approximations oscillating in  $[0, T) \times (-\epsilon, \epsilon)$  will lead to larger values of  $\|f(\tilde{u})_x\|_{\infty}$ , showing that the goal functional penalizes spurious oscillations.

**Remark 2.** *The above arguments were outlined only in the case of a stationary shock. However, the arguments can be adapted to cover moving shocks. The estimates employed are done pointwise for each  $t \in [0, T)$ , such that the only difference is that the interval  $(-\epsilon, \epsilon)$  now moves with the proper shock velocity instead of being fixed.*

The wPINN approach fits into the previous analysis. It introduces a (Kruzhkov) *entropy residual* [17], based on enforcing entropy inequalities, which is then turned into a loss function by measuring it in something similar to the  $L^2$ - $H^{-1}$  norm. For  $\bar{S} := \{\varphi \in C_c^\infty([0, T) \times D) : \varphi \geq 0, \|\partial_x \varphi\|_{L^2([0, T) \times D)} = 1\}$ , the loss function on the continuous level is given by

$$\mathcal{L}_{\text{ent}}^K(u_\theta) = \sup_{\varphi \in \bar{S}} \max_{c \in \mathbb{R}} \int_{[0, T)} \int_D \varphi \partial_t |u_\theta - c| - \text{sign}(u_\theta - c)(f(u_\theta) - f(c)) \varphi_x \, dx \, dt. \quad (22)$$

Note that this form of loss contains a nested maximization problem over  $c \in \mathbb{R}$ , which is approximated in [17] by sampling some discrete set of  $c$  and computing the maximum directly.

In contrast to our previous arguments,  $\mathcal{L}_{\text{ent}}^K$  is not based on computing a norm of the PDE residual directly, however the entropies already encode the PDE itself. Being based on entropy conditions, this choice of loss ensures that one finds the unique entropy solution. Conventional PINNs approach this by viscous regularization instead, see [2].

**2.4. A Variant of wPINNs — Motivation.** Our method aims to improve the computational efficiency of the wPINN strategy. Indeed, we approach both enforcement of the entropy condition and the weak norm estimation differently to accelerate learning in terms of the number of epochs the neural networks require to be trained to comparable accuracy, or achieve higher accuracy at equal points in training.

The first major change we make to the wPINN method is that we use the PDE residual function measured in the  $L^2$ - $H^{-1}$  norm instead of the Kruzhkov entropy residual employed previously. Recall that  $S = \{\varphi \in V : \|\varphi\|_V = 1\}$  with  $V = H_0^1(D)$ . The interior PDE residual loss is then given by

$$\mathcal{L}_{\text{int}}^u(u_\theta) = \int_{[0, T)} \left( \sup_{\varphi \in S} \int_D (\partial_t u_\theta + \partial_x u_\theta) \varphi \, dx \right)^2 dt. \quad (23)$$

This loss does not guarantee that one always finds the entropy solution anymore. However, provided  $f$  is strictly convex, one is free to use any single strictly convex entropy-entropy flux pair instead of the family of Kruzhkov entropies to enforce entropy admissibility. Thus, we fix one such entropy-entropy flux pair  $(\eta, q)$  and introduce the *entropy loss*, measured in the  $L^2$ - $H^{-1}$  norm, as

$$\mathcal{L}_{\text{ent}}^\eta(u_\theta) = \int_{[0, T)} \left( \sup_{\xi \in S} \int_D (\eta(u_\theta)_t + q(u_\theta)_x)^\oplus \xi \, dx \right)^2 dt, \quad (24)$$

where  $(\cdot)^\oplus$  denotes the positive part of a function. By using the positive part, we enforce the entropy condition as an inequality. This approach avoids the nested maximization over  $c \in \mathbb{R}$  of the original wPINN approach in favor of a second, independent, maximization problem with another adversarial neural network that one approximates with gradient ascent.

The second major change we make lies in the estimation of the  $H^{-1}$  norm. When using the straightforward definition, one takes a supremum over all  $\varphi \in H_0^1(D)$  with  $\|\varphi\|_{H^1(D)} = 1$ . If one now parameterizes approximations to  $\varphi$  using a neural network, it is unclear how to enforce the normalization of the test function through the network design, so one has to compute the  $H^1$  norm (using Monte-Carlo methods) and divide by this. We believe that the division by such a

norm makes the maximization problem more difficult. Also, by construction, this formulation is invariant under scalar rescaling of the norm approximation network. As parts of the updates during the gradient ascent process however change the overall normalization of the network, this undetermined degree of freedom may reduce the speed and accuracy of the norm estimation.

To remedy these downsides, we propose computing the  $H^{-1}$  norm instead by learning the solution to a dual elliptic problem. Given a functional  $v \in H^{-1}(D)$ , by identifying the dual space  $(H^{-1}(D))' = H_0^1(D)$ , we see that solving

$$\text{Find } w \in H_0^1(D) \text{ with } \int_D \nabla w \nabla \zeta \, dx = \int_D v \zeta \, dx \quad \text{for all } \zeta \in H_0^1(D), \quad (25)$$

one has  $\|v\|_{H^{-1}(D)}^2 = \|w\|_{H^1(D)}^2 := \|\nabla w\|_{L^2(D)}^2$ . Note that due to the zero-boundary conditions, by Poincaré inequality the  $H^1$ -seminorm is a proper norm. This dual elliptic problem is easily solved using the “Deep Ritz Method” [26], that is by maximizing the functional

$$I(w) = \int_D v w \, dx - \frac{1}{2} \int_D |\nabla w|^2 \, dx. \quad (26)$$

The maximization is known to be robust and effective even for low-regularity right-hand-sides  $v$  for the Poisson problem [38].

**2.5. Loss Definition.** To apply these concepts on the discrete level, we choose sets of random collocation points for initial condition, boundary condition and interior of the domain:

- Interior collocation points  $S_{\text{int}} := \{t_i, x_i\}_{i=1}^{N_{\text{int}}}$  with  $t_i \in [0, T)$  and  $x_i \in D$  and  $N_{\text{int}}$  the number of collocation points.
- Initial collocation points  $S_{\text{ic}} := \{0, x_i\}_{i=1}^{N_{\text{ic}}}$  with  $x_i \in D$  and  $N_{\text{ic}}$  the number of collocation points.
- Boundary collocation points  $S_{\text{bc}} := \{t_i, x_i\}_{i=1}^{N_{\text{bc}}}$  with  $t_i \in [0, T)$  and  $x_i \in \partial D$  and  $N_{\text{bc}}$  the number of collocation points.

We work with three neural networks  $u_\theta$ ,  $\tilde{\varphi}_\chi$  and  $\tilde{\xi}_\nu$  with weights denoted by  $\theta, \chi$  and  $\nu$ . The latter two networks are used to approximate the solutions to the dual problems as above, so one needs to enforce zero boundary conditions through either soft- or hard constraints [38]. Soft constraints add an additional loss term penalizing the violation of boundary conditions. Hard constraints encode the boundary condition exactly into the network design. We opt for hard constraints, because this speeds up learning and improves accuracy of PINNs [38]. We implement the boundary conditions through a cutoff function  $w : D \rightarrow \mathbb{R}^+$  with  $w|_{\partial D} = 0$ ,  $w'|_{\partial D} \neq 0$  and  $w(x) > 0$  for all  $x$  in the interior of  $D$ . In the following we refer to  $\varphi_\chi(x, t) := \tilde{\varphi}_\chi(x, t)w(x)$  and  $\xi_\nu(x, t) := \tilde{\xi}_\nu(x, t)w(x)$  as the corresponding neural networks satisfying the boundary conditions instead.

To simplify notation we define

$$\mathcal{r}_{\text{int}}(u_\theta; \varphi_\chi) := (\partial_t u_\theta) \varphi_\chi - f(u_\theta) (\partial_x \varphi_\chi). \quad (27)$$

This definition corresponds to the integrand of the PDE residual loss after integration by parts in space, as the boundary contributions vanish because the network  $\varphi_\chi$  has zero boundary conditions in space. The integration by parts when defining the loss for numerical simulations is also done in [17] and gives good results, so we adopt this approach as well. The overall PDE residual loss is then discretized as

$$\mathcal{L}_{\text{int}}^u := \frac{1}{N_{\text{int}}} \left( \sum_{S_{\text{int}}} \mathcal{r}_{\text{int}}(u_\theta; \varphi_\chi)(t_i, x_i) - \frac{1}{2} |\nabla_x \varphi_\chi|^2(t_i, x_i) \right). \quad (28)$$

We solve the elliptic problem in space using a single network with the time  $t$  as an additional input parameter, such that it learns the solution for the dual problem simultaneously on the entire time interval. This is equivalent to the continuous definition of the loss, but more effective on the discrete level.

Note that, when  $\varphi_\chi$  (approximately) solves the aforementioned dual elliptic problem for the PDE residual as a right-hand side, (28) corresponds to the Monte-Carlo approximation of  $\frac{1}{2} \int_{[0,T)} \int_D |\nabla_x \varphi_\chi|^2 dx dt$ . We compute the approximation in this form because the dependence on the parameters  $\theta$  of the network  $u_\theta$  is straightforward then.

Further, we have the *entropy residual* for a given entropy-entropy flux pair  $(\eta, q)$  defined as

$$\mathcal{r}_{\text{ent}}(u_\theta; \xi_\nu; (\eta, q)) := (\eta(u_\theta)_t + q(u_\theta)_x)^\oplus \xi_\nu, \quad (29)$$

which we measure again in the squared  $L^2$ - $H^{-1}$  norm as

$$\mathfrak{L}_{\text{ent}}^\eta := \frac{1}{N_{\text{int}}} \left( \sum_{S_{\text{int}}} \mathcal{r}_{\text{ent}}(u_\theta; \xi_\nu)(t_i, x_i) - \frac{1}{2} |\nabla_x \xi_\nu|^2(t_i, x_i) \right). \quad (30)$$

Putting these parts together we consider the following interior loss function:

$$\mathfrak{L}_{\text{int}} = \mathfrak{L}_{\text{ent}}^\eta + \mathfrak{L}_{\text{int}}^u \quad (31)$$

Note that the interior loss consists of two additive contributions, the PDE residual loss (28) and the entropy loss (30), each of which again consist of two parts. The PDE residual loss  $\mathfrak{L}_{\text{int}}^u$  has no dependence on the adversarial network  $\xi_\nu$ , and the spatial gradient part depends only on the network  $\varphi_\chi$ , while the entropy loss  $\mathfrak{L}_{\text{ent}}^\eta$  does not depend on  $\varphi_\chi$  and its spatial gradient part depends only on  $\xi_\nu$ .

For the overall loss we add in initial- and boundary contributions, for Dirichlet boundary data  $g$  on the spatial boundary of the domain and initial data  $u_0$  at  $t = 0$ . This gives the overall loss function

$$\begin{aligned} \mathfrak{L}(u_\theta, \varphi_\chi, \xi_\nu) &= \mathfrak{L}_{\text{int}}(u_\theta, \varphi_\chi, \xi_\nu) \\ &+ \lambda \left( \frac{1}{N_{\text{ic}}} \sum_{S_{\text{ic}}} (u_\theta(0, x_i) - u_0(0, x_i))^2 + \frac{1}{N_{\text{bc}}} \sum_{S_{\text{bc}}} (u_\theta(t_i, x_i) - g(t_i, x_i))^2 \right), \end{aligned} \quad (32)$$

with parameter  $\lambda > 0$ . These additional terms depend only on the solution network  $u_\theta$ . The decomposition of the loss into additive terms independent of some of the networks allows avoiding some computations to improve efficiency. For example, computing a gradient of the loss with respect to only the parameters  $\theta$  does not require computation of the spatial gradients of the networks  $\varphi_\chi$  and  $\xi_\nu$  in (28) and (30). The parameter  $\lambda$  may be chosen to balance gradients of the interior and boundary contributions during training [39].

### 3. ALGORITHM AND IMPLEMENTATION DETAILS

In this section we assemble the previously discussed loss function into a full neural-network training procedure. Additionally we discuss the importance and use of several hyperparameters in training and outline optimization techniques used in our numerical experiments and extensions one may consider.

**Algorithm 1** Neural Network Training algorithm

---

**Input:** Initial data  $u_0$ , boundary data  $g$ , flux function  $f$ , strictly convex entropy-entropy flux pair  $(\eta, q)$ , Hyperparameters:  $\tau_{\min}, \tau_{\max}, N_{\max}, \lambda, \gamma$

**Output:** Best networks  $u_{\theta}^b, \varphi_{\chi}^b, \xi_{\nu}^b$

- 1: Initialize the networks  $u_{\theta}, \varphi_{\chi}, \xi_{\nu}$
- 2: Initialize performance metric  $\mathcal{L}_{\text{avg}} \leftarrow \mathcal{L}(u_{\theta}, \varphi_{\chi}, \xi_{\nu})$
- 3: Initialize best performance metric  $\mathcal{L}_{\text{best}} \leftarrow \infty$
- 4: Generate collocation points  $S_{\text{int}}, S_{\text{ic}}, S_{\text{bc}}$
- 5: **for**  $ep = 1, \dots, N_{\text{ep}}$  **do**
- 6:     **for**  $k = 1, \dots, N_{\max}$  **do**
- 7:         Compute  $\mathcal{L}(u_{\theta}, \varphi_{\chi}, \xi_{\nu})$
- 8:         Update  $\chi \leftarrow \chi + \tau_{\max} \nabla_{\chi} \mathcal{L}(u_{\theta}, \varphi_{\chi}, \xi_{\nu})$
- 9:         Update  $\nu \leftarrow \nu + \tau_{\max} \nabla_{\nu} \mathcal{L}(u_{\theta}, \varphi_{\chi}, \xi_{\nu})$
- 10:     **end for**
- 11:     Compute  $\mathcal{L}(u_{\theta}, \varphi_{\chi}, \xi_{\nu})$
- 12:     Update  $\theta \leftarrow \theta - \tau_{\min} \nabla_{\theta} \mathcal{L}(u_{\theta}, \varphi_{\chi}, \xi_{\nu})$
- 13:     Update performance indicator  $\mathcal{L}_{\text{avg}} \leftarrow (1 - \gamma) \mathcal{L}_{\text{avg}} + \gamma \mathcal{L}(u_{\theta}, \varphi_{\chi}, \xi_{\nu})$
- 14:     **if**  $\mathcal{L}_{\text{avg}} < \mathcal{L}_{\text{best}}$  **then**
- 15:          $\mathcal{L}_{\text{best}} \leftarrow \mathcal{L}_{\text{avg}}$
- 16:         Save best networks  $u_{\theta}^b, \varphi_{\chi}^b, \xi_{\nu}^b \leftarrow u_{\theta}, \varphi_{\chi}, \xi_{\nu}$
- 17:     **end if**
- 18: **end for**

---

**3.1. Training Algorithm.** Our training procedure is described in Algorithm 1. It is essentially a standard generative adversarial neural network (GAN) training procedure including best model checkpoints, and as such many of the usual heuristics in the training of such network architectures apply. We comment on our checkpoint procedure briefly in the following section.

Note that lines 7 and 11 of the algorithm compute the loss function depending on the networks. These steps provide the computational graphs to backpropagate gradients using automatic differentiation for the following update steps. We write these steps to represent a practical implementation in machine learning frameworks.

**Remark 3.** *In Algorithm 1, we use a simple set of hyperparameters to reduce expositional complexity. In practice, for the examples we studied, this set of hyperparameters is sufficient to achieve effective and stable training, however this may not always be the case. Particularly, it is generally unclear whether both the estimation networks  $\varphi_{\chi}$  and  $\xi_{\nu}$  should use the same learning rate. If learning proves difficult for any of these networks one should consider using separate learning rates and number of maximization steps for either.*

**3.2. Implementation Notes.** We now outline some common and useful heuristics in training such network architectures.

**3.2.1. Gradient Descent Algorithms.** In the general algorithm 1, for simplicity, we describe regular gradient descent weight updates. Instead, any other gradient-based optimization algorithm may be used to update the weights. We have experienced good results using the Adam algorithm [40] and its AMSGrad variant [41], which are both extremely popular choices for training neural networks due to their oftentimes faster minimization of the training loss.

**3.2.2. Efficient Loss Computation.** While we think of  $\mathcal{L}(u_\theta, \varphi_\chi, \xi_\nu)$  as the loss function used for minimization with respect to  $u_\theta$  and maximization with respect to  $\varphi_\chi$  and  $\xi_\nu$ , one does not need to compute the entire loss for each of the optimization steps. As discussed during the definition of our loss (32), it possesses an additive decomposition into several parts depending only on one or two networks. We do not compute parts of the loss when they do not contribute to the gradients for weight updates.

**3.2.3. Learning Rates- and Scheduling.** The learning rates  $\tau_{\min}$  and  $\tau_{\max}$  play an important role in training and choosing them adequately has a big impact on both training time and resulting network parameters. On the one hand, larger learning rates are desirable because larger gradient descent steps require less overall steps, but on the other hand, because the loss function is typically non-convex, using a large and fixed learning rate often results in worse final network configurations even when the update is stable.

Instead of fixed learning rates, it is common to vary the learning rate during training using “learning rate scheduling”. It is typical to start with a large initial learning rate and then reduce it over the course of training, commonly by one or more orders of magnitude as training progresses. Further, one may “cycle” learning rates in a schedule [42], that is, intermittently increase the learning rate again to attempt to escape local minima or speed up training when the network is in a “plateau” in the loss landscape which is slow to traverse with small learning rates.

In our experience, cyclical learning rate scheduling was very effective at obtaining more precise results. However, our numerical experiments only use a basic linear learning rate schedule to match the implementation of the original wPINNs [17].

**3.2.4. Network Checkpointing.** An important technique during the training of neural networks is *checkpointing*, i.e. saving well-performing neural network weights and returning these instead of the final weights obtained after all training epochs are completed.

As a heuristic for determining network performance, one option is the neural network loss. We do not choose the loss directly but rather track an exponential average  $\mathfrak{L}_{\text{avg}}$  decaying at a rate of  $1 - \gamma$ , where  $\gamma \in (0, 1)$  is some parameter one is free to choose. Updating the performance indicator  $\mathfrak{L}_{\text{avg}}$  is done using the loss from before the weight update to  $u_\theta$ , however typical update steps only change this quantity slightly per epoch and doing so avoids one additional loss computation per epoch, making this convenient in practice.

The exponential averaging is non-standard, however we believe it is more sensible in this setting than just tracking the epoch loss directly. Our reasoning for choosing to save model configurations based on the exponentially averaged loss is that in this adversarial setting, the solution network  $u_\theta$  may update its weights in a fashion that confuses the adversarial networks, such that they grossly underestimate the correct value of the loss briefly during some maximization steps. This leads to several epochs where the loss is low and the solution network then performs a few bad weight updates before the adversarial networks recover and give accurate estimations again. Afterwards, one correctly observes an increased loss due to the poor weight updates of previous iterations.

Thus, it is disadvantageous to save single epochs where the loss is lowest, because this favors saving networks where the adversarial networks are not working properly. Tracking an exponential average of the loss mitigates this issue, leaving only the desired property of the averaged loss decreasing as the approximation to the solution improves, when the adversarial networks are working well.

**Remark 4** (A-Posteriori Performance Indicator). *The previous section on network checkpoints covers only a heuristic that, while useful in practice, has no rigorous theoretical basis, i.e. there is no guarantee that the neural networks one obtains are close to the true solution. On the other hand, rigorous theoretical a-priori bounds based on the Kruzhkov entropy loss were derived in [17].*

*For a fixed solution network  $u_\theta$  which one obtains from our (or any other) training procedure, one may compute the adversarial network for the Kruzhkov entropy loss by performing several gradient ascent steps.*

*The Monte-Carlo approximation of the Kruzhkov entropy loss then provides a theoretically founded error indicator that can be used in ensemble training or during checkpointing, instead of the training loss, to select the best networks in an ensemble. If this is only done intermittently as a post-processing step, the numerical effort for this step is low compared to the overall training costs.*

#### 4. NUMERICAL RESULTS

In this section we present several numerical experiments to compare the performance of our modified method against the original wPINN method. We train neural networks for initial data corresponding to a standing shock, a moving shock, a rarefaction wave from Riemann problem initial data and sine initial data, to match the range of examples covered in [17].

**4.1. Comparison Setup.** In this section we describe our general methodology for comparing the performance of the original wPINN algorithm and our modified algorithm as described previously.

As a target metric for comparing algorithm performance we study the relative space-time  $L^1$  error of approximate solutions given by

$$\mathcal{E}_r(u_\theta) = \frac{\int_{[0,T] \times D} |u_\theta(t, x) - u(t, x)| \, dx \, dt}{\int_{[0,T] \times D} |u(t, x)| \, dx \, dt}, \quad (33)$$

where  $u$  denotes the true solution, because it is straightforward to compute and is also used in [17], so we can verify that we accurately portray the original wPINN performance by cross-referencing results therein. The integrals are approximated using Monte-Carlo integration with  $2^{17}$  points in the space-time domain. In cases where there is no closed-form analytical expression for  $u$ , we approximate it using a high-resolution finite volume scheme as provided by the PyClaw python package [43].

We perform an ensemble training procedure as in [17], however we do not investigate as large a range of hyperparameters. Instead, we try several hyperparameter configurations until we find parameters that give good results for the original wPINN algorithm and then use the exact same hyperparameters for training both approaches. Importantly this means using the exact same width and number of layers as well as learning rate for the network approximating the solution. Although there is no direct corresponding network for  $\xi_\nu$  in the original wPINN approach, we match this network's hyperparameters to those of  $\varphi_\chi$ . This keeps the two training procedures as comparable as possible.

As a learning rate schedule, we reduce the learning rate linearly by half over the total number of epochs. While we think that a more aggressive learning rate schedule would benefit our modified approach, to be able to check our results against the original wPINN results from [17] we choose to keep this setting unmodified.



TABLE 1. Relative error  $\mathcal{E}_r(u^*)$  of the average network prediction at the final epoch of training.

	original	modified
Standing shock	$2.99 \cdot 10^{-3}$	$3.02 \cdot 10^{-3}$
Moving shock	$1.46 \cdot 10^{-2}$	$1.36 \cdot 10^{-2}$
Rarefaction Wave	$1.45 \cdot 10^{-2}$	$1.18 \cdot 10^{-2}$
Sine Wave	$5.03 \cdot 10^{-2}$	$1.19 \cdot 10^{-2}$

For both algorithms we track  $\mathcal{E}_r(u_\theta)$  for each network of the ensemble individually over the training epochs for comparison, sampled at multiple points during training.

Additionally, we also compare the quality of the *average network* predictions

$$u^*(t, x) = \frac{1}{N^*} \sum_{i=1}^{N^*} u_{\theta,i}(t, x), \quad (34)$$

for an ensemble  $\{u_{\theta,i}\}_{i=1}^{N^*}$  consisting of  $N^*$  neural networks trained for the same hyperparameters, but different randomly chosen initial layer weights and biases. We compute  $\mathcal{E}_r(u^*)$  only at the final epoch of training.

**4.2. Standing Shock.** We begin by considering the Burgers equation on  $[0, 0.5) \times [-1, 1]$  for the initial datum

$$u_0(x) = \begin{cases} 1 & \text{for } x \leq 0, \\ -1 & \text{for } x > 0, \end{cases} \quad (35)$$

The corresponding solution is given by

$$u(t, x) = \begin{cases} 1 & \text{for } x \leq 0, \\ -1 & \text{for } x > 0, \end{cases} \quad (36)$$

that is, a standing shock at  $x = 0$ .

We use the following hyperparameters which are the same for both procedures:  $\tau_{\min} = 0.01$ ,  $\tau_{\max} = 0.015$ ,  $N_{\max} = 8$ ,  $N_{\text{ep}} = 1000$ . The networks  $u_\theta$  in both algorithms have  $l_\theta = 6$  layers of width  $w_\theta = 20$  with  $\sigma_\theta(\cdot) = \tanh(\cdot)$  activation. The networks  $\varphi_\chi$  and  $\xi_\nu$  use 4 layers of width 10 with tanh activation function in either algorithm.

We fix the convex entropy-entropy flux pair  $\eta(u) = \frac{1}{2}u^2$  and  $q(u) = \frac{1}{3}u^3$  for all following examples.

For the original wPINNs we adopt the penalty parameter  $\lambda = 10$ , as fixed during the numerical experiments in [17], while for our method  $\lambda = 1$  seems to work better. Because we use different loss functions it is not sensible to keep this parameter matched. We set  $\gamma = 0.3$  for the exponential averaging of past loss values. The original wPINN algorithm also requires a choice of reset frequency for the adversarial network which we choose as  $r_f = 0.05$ . Lastly, we compute  $N^* = 16$  retrainings.

In both algorithms we use  $N_{\text{int}} = 16384$  uniformly randomly sampled interior collocation points,  $N_{\text{ic}} = 4096$  initial collocation points and  $N_{\text{bc}} = 4096$  boundary collocation points. These points are randomly chosen anew for each retraining of neural networks and choice of algorithm, however stay fixed during the training of each single network.

We plot the results for the standing shock in Figure 1a. The error bars show the standard error of the mean, that is  $\frac{\sigma}{\sqrt{N^*}}$  with  $\sigma$  the standard deviation of the relative  $L^1$  errors in the

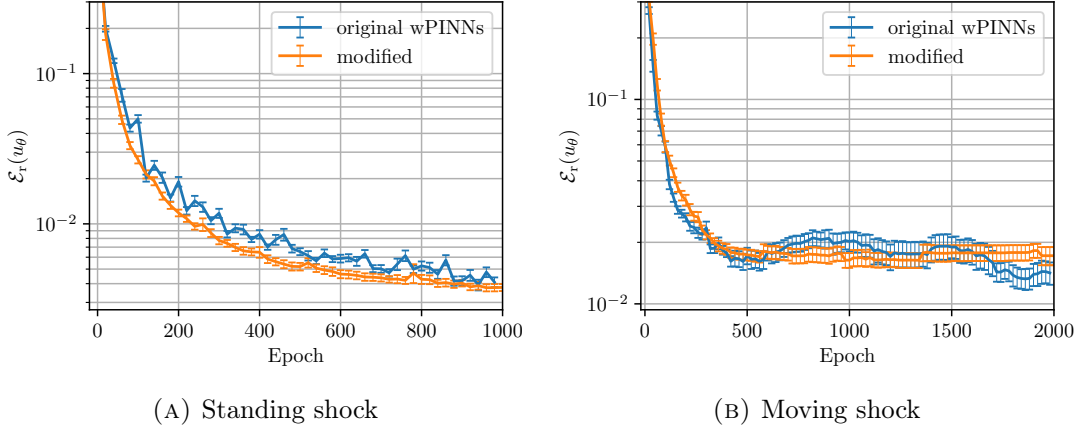


FIGURE 1. Evolution of the mean value and standard error of  $\mathcal{E}_r$  for the respective network ensembles.

ensemble. In this example we see that the performance of both methods is approximately equally good. We list the average network prediction error in Table 1. In particular, the table shows that we reproduce the accuracy achieved in the numerical experiments of [17].

There are a few small differences in the evolution of  $\mathcal{E}_r$ , such as our approach giving a “smoother” evolution of the relative error over the epochs and having generally smaller statistical errors.

We attribute the smoother measurements of the relative error to more stable norm estimation of our loss functional by avoiding the division by the  $H^1$ -seminorm of the approximating network and possibly the adjusted checkpointing procedure as well.

Confirming our expectations, we see that both training procedures perform well, showing that both methods are suitable for approximating shock solutions. We think the difference between the two methods is small in this example because this is a very easy benchmark problem. As the initial data is already a shock, the  $L^2$ -norm based loss contributions from initial and boundary data heavily influence the overall learning of the solution profile. The additional PDE residual contribution now only needs to ensure that the shock is placed at the right position, and because the shock is stationary this is straightforward, giving only a small contribution to the total loss.

The initial- and boundary terms are identical in both algorithms. During training one can check that the majority of the overall loss for either algorithm is due to these contributions, and because the Adam algorithm for minimizing the loss is invariant with respect to scalar rescaling of the entire loss, also the different choice of penalty parameter  $\lambda$  has only minor influence on the training procedure. This makes it plausible that one does not observe any real improvement over the standard wPINN algorithm in this example.

**4.3. Moving Shock.** For completeness sake, we also consider a moving shock example. We choose

$$u_0(x) = \begin{cases} 1 & \text{for } x \leq 0, \\ 0 & \text{for } x > 0. \end{cases} \quad (37)$$

as an initial datum leading to the solution

$$u(t, x) = \begin{cases} 1 & \text{for } x \leq \frac{t}{2}, \\ 0 & \text{for } x > \frac{t}{2}, \end{cases} \quad (38)$$

which is a moving shock starting from  $x = 0$ , moving to the right with a speed of 0.5.

We choose the same training setup and hyperparameters as for the standing shock with the exception that we train the moving shock for  $N_{\text{ep}} = 2000$  epochs instead. Note that keeping the reset frequency in the original wPINN algorithm fixed while changing the number of epochs means that the number of epochs between two resets of the adversarial network changes.

As expected, the results for this example are structurally the same as in the standing shock example. We plot the results for the moving shock in Figure 1b, and reference the average network prediction error in Table 1.

The individual and averaged errors are slightly larger for this example, but again the errors we get are in line with the expectations from the original wPINN experiments.

The rest of the discussion is analogous to the standing shock. However, because the shock is moving at a constant velocity, the PDE residual now essentially amounts to learning a single linear transformation to ensure correct placement of the solution profile learned from the initial data. This is slightly less straightforward than previously, resulting in a larger relative error, but still works well and gives only a small contribution to the total loss.

**4.4. Rarefaction Wave.** As another prototypical example, we consider a rarefaction wave on  $[0, 0.5) \times [-1, 1]$  for the initial data

$$u_0(x) = \begin{cases} -1 & \text{for } x \leq 0, \\ 1 & \text{for } x > 0. \end{cases} \quad (39)$$

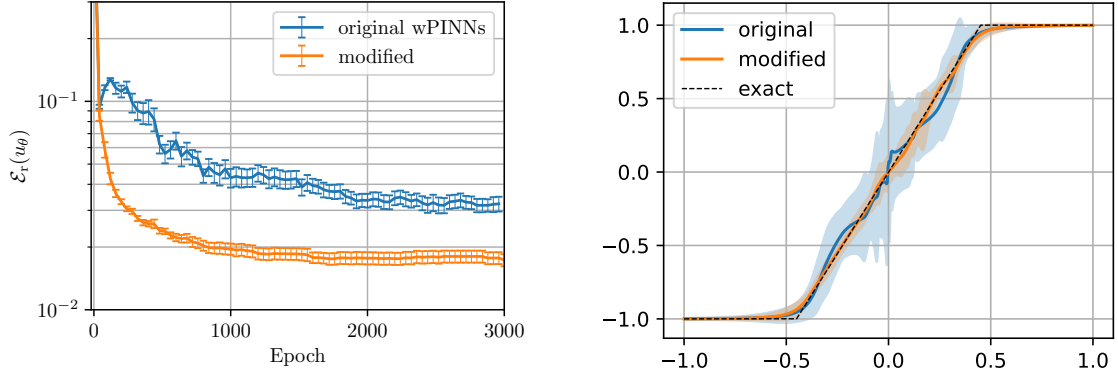
For this, the exact solution is given by a rarefaction wave

$$u(t, x) = \begin{cases} -1 & \text{for } x \leq -t, \\ \frac{x}{t} & \text{for } -t < x \leq t, \\ 1 & \text{for } x > t. \end{cases} \quad (40)$$

This example is illustrative of situations where, without additional entropy conditions, solutions are non-unique and will show that our strategy for enforcing entropy conditions works. We train our neural networks for this example using the same hyperparameters as in the previous examples, except that we train for a total of  $N_{\text{ep}} = 3000$  epochs now.

The mean relative error of the ensemble as training progresses is shown in Figure 2a. For the average network prediction, the original wPINN algorithm gives a relative error of  $\mathcal{E}_r(u_{\text{orig}}^*) = 1.45 \cdot 10^{-2}$ . This is comparable with the results published in [17]. Our method gives a relative error of  $\mathcal{E}_r(u_{\text{mod}}^*) = 1.18 \cdot 10^{-2}$  instead.

Because this example is no longer dominated by how quickly the network can learn the correct shape of the solution from the initial datum, it is better-suited to illustrate the advantages of our method. In this example we see that our method provides a sizable advantage over the original wPINN algorithm. As shown in Fig. 2a, the individual wPINN network predictions have, on average, a  $3.2\% \pm 0.26\%$  relative error at the final epoch while the modified algorithm has an error of only  $1.7\% \pm 0.12\%$ , which is a reduction of the individual network error by slightly less than half. Our method also gives a more precise average prediction, with an about 20% reduction in the overall relative error. The larger reduction of error in the individual network predictions



(A) Evolution of the mean value and standard error of  $\mathcal{E}_r$  for the respective network ensembles.

(B) Comparison of average network predictions for original and modified wPINNs at  $t = 0.45$  after  $N_{ep} = 3000$  epochs. Shaded bands are  $2\sigma$ -standard deviations of the average network prediction.

FIGURE 2. Rarefaction wave with shock initial data

may indicate that smaller ensembles suffice to produce consistently good approximations of the true solution for our algorithm.

We observe that our modified algorithm produces a smoother epoch series of the mean relative error for this example as well. Our algorithm produces significantly better approximations, especially early into the training process, producing approximations that are comparable with the final estimation quality after as little as 1000 epochs. The original wPINN algorithm takes longer for the relative error to plateau on its final value.

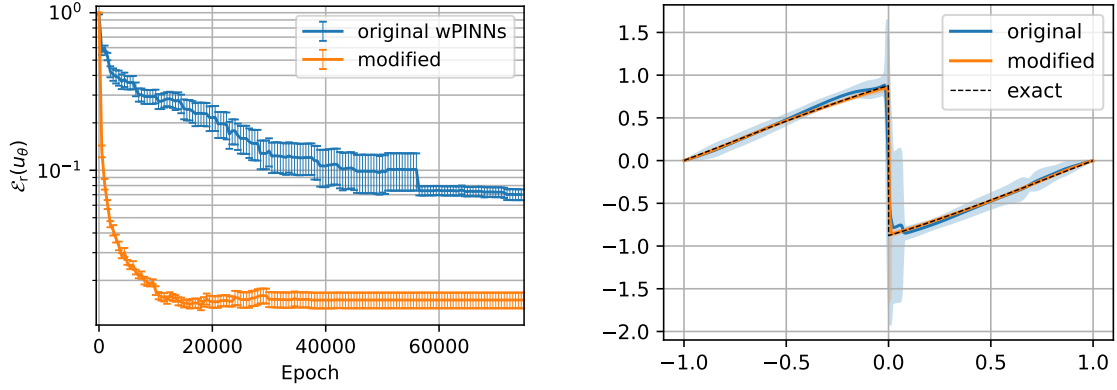
In Figure 2b we show the ensemble averaged prediction at the end of training for the original and modified wPINN algorithm at  $t = 0.45$ . We see several striking differences. The original wPINN algorithm produces spurious oscillations when approximating the solution to this problem. While both the modified loss and the original wPINN loss penalize spurious oscillations as argued in Section 2, we observe that the modified approach seems to penalize this more effectively, so we do not observe significant oscillations for its results. Additionally the standard deviation for the average network predictions is significantly larger for the original wPINN algorithm than that of our modified approach. Notably, the error bands are widest for the original wPINNs at  $x = 0$ , where the discontinuity is at in the initial data. This is not the case for the results from [17] and we do not completely understand why this occurs, but it may be related to original wPINNs using sin activation functions instead of tanh.

**4.5. Sine Wave.** Lastly we consider the Burgers equation for sine initial data  $u_0(x) = -\sin(\pi x)$  on  $[0, 1] \times [-1, 1]$  and  $u(t, -1) = u(t, 1) = 0$  for  $t \in [0, T]$ . This example is significantly more challenging to solve to high precision using neural networks, because unlike previous examples we have smooth initial data and subsequent shock formation inside the computational domain. This means the network approximation has to steepen over time, developing into a shock separating two rarefactions. This example is also studied in [17].

Because this example is more challenging, and to reproduce the simulation setup in [17], instead of uniformly randomly sampled points on the domain we use low-discrepancy Sobol points.

These approximate the numerical integrals more precisely than previous uniformly randomly sampled points, improving network performance.

In our preliminary experiments we find the hyperparameter choices from the previous two examples to perform best for the original wPINN algorithm again, but because the underlying solution is significantly more complicated we increase the number of epochs to  $N_{\text{ep}} = 75000$ . Because we train for significantly more epochs, we also reduce  $\gamma$  to 0.015 for the exponential loss averages.



(A) Evolution of the mean value and standard error of  $\mathcal{E}_r$  for the respective network ensembles.

(B) Comparison of average network predictions for original and modified wPINNs at  $t = 0.75$  after  $N_{\text{ep}} = 75000$  epochs. Shaded bands are  $2\sigma$ -standard deviations of the average network prediction.

FIGURE 3. Sine initial data

As before, we show the mean relative error of the ensemble over the training epochs in Figure 3a. In this challenging example we see a very noticeable difference between the original and the modified wPINN algorithms. The mean value of  $\mathcal{E}_r$  at the final training epoch for the original wPINNs is  $7.0\% \pm 0.6\%$ , while the modified algorithm gives a mean relative error of only  $1.5\% \pm 0.17\%$ . The drop in the mean relative error for the original wPINNs after about 55000 epochs alongside a large reduction in the standard error is due to a single poorly-performing outlier network improving to match the performance of the remaining ensemble at this point in training. This is very visible given the limited ensemble size of  $N^* = 16$  retrainings.

The average network predictions are compared in Figure 3b. The original wPINNs have a relative error of  $\mathcal{E}_r(u_{\text{orig}}^*) = 5.03 \cdot 10^{-2}$ , which is larger but comparable to the results from [17]. For our modified algorithm we find  $\mathcal{E}_r(u_{\text{mod}}^*) = 1.19 \cdot 10^{-2}$  instead, which is better than the results from [17]. We see the same structural differences in the average network predictions as with the rarefaction example, that is, significantly larger standard deviation of the average network prediction and (mild) spurious oscillations for the original wPINNs.

Note that for our modified algorithm, this final level of accuracy is roughly in line with the previous example, with the main difference being that it takes more epochs to reach this level of accuracy. In our tests we saw that increasing the number of collocation points and choosing a different learning rate schedule can further improve results, while the networks themselves appear to be able to approximate the solution of the underlying problem to higher accuracy without

changing the network size, indicating that these hyperparameters restrict the final precision most for our examples.

## 5. DISCUSSION

Approximating nonlinear hyperbolic conservation laws using conventional PINNs is not straightforward and may fail when the PDE exhibits discontinuous solutions. The wPINN strategy from [17] enables the accurate approximation of entropy solutions to scalar conservation laws. The main reason wPINNs are effective for this type of problem is that they compute a weak norm of the PDE residual by parametrizing test functions with neural networks, leading to an adversarial min-max problem structure which may be solved with standard deep learning techniques.

One of the main shortcomings of wPINNs is that their training is more computationally expensive than that of conventional PINNs, because of the min-max problem structure.

We modify several core parts of the original wPINN algorithm to make training more efficient. In the original wPINN algorithm, the Kruzhkov entropy residual has two important roles: enforcing the PDE in a weak sense and selecting the entropy solution. We split these roles into separate terms by introducing a PDE loss and an entropy loss with respect to a convex entropy-entropy flux pair. This gives more flexibility to both terms. Crucially, this means we do not have to use the Kruzhkov family of entropies and can opt for a smoother entropy, which makes training easier.

For both these loss contributions we also change how we approximate their respective weak norms. Instead of using the supremum-based definition for such norms, which involves normalization of the test function, we reformulate the norm computation via the solution of a dual elliptic problem. While this still leads to a min-max formulation of the loss, it has a simpler structure that makes the training process easier.

In numerical experiments we illustrate the benefits of our modifications. Especially for more challenging problems we see large improvements expressed by lower mean relative errors after the same number of training epochs and better approximations at the end of training. In the numerical experiments, we match our training procedure as faithfully as possible between both methods to ensure that the comparison is fitting and, indeed, this reproduces the results for original wPINNs from [17]. Thus, the hyperparameters that were chosen are not tuned to show the best performance our modified method is capable of and doing so may achieve even better results.

## REFERENCES

- [1] M. Raissi and G. E. Karniadakis, “Hidden physics models: Machine learning of nonlinear partial differential equations”, *Journal of Computational Physics*, vol. 357, pp. 125–141, 2018, ISSN: 0021-9991.
- [2] M. Raissi, P. Perdikaris, and G. E. Karniadakis, “Physics-informed neural networks: A deep learning framework for solving forward and inverse problems involving nonlinear partial differential equations”, *Journal of Computational Physics*, vol. 378, pp. 686–707, 2019.
- [3] K. O. Lye, S. Mishra, and D. Ray, “Deep learning observables in computational fluid dynamics”, *Journal of Computational Physics*, vol. 410, p. 109339, 2020.
- [4] L. Yang, X. Meng, and G. E. Karniadakis, “B-PINNs: Bayesian physics-informed neural networks for forward and inverse PDE problems with noisy data”, *Journal of Computational Physics*, vol. 425, p. 109913, 2021, ISSN: 0021-9991.
- [5] M. Dissanayake and N. Phan-Thien, “Neural-network-based approximations for solving partial differential equations”, *Communications in Numerical Methods in Engineering*, vol. 10, no. 3, pp. 195–201, 1994.
- [6] I. Lagaris, A. Likas, and D. Papageorgiou, “Neural-network methods for boundary value problems with irregular boundaries”, *IEEE Transactions on Neural Networks*, vol. 11, no. 5, pp. 1041–1049, 2000.

- [7] I. Lagaris, A. Likas, and D. Fotiadis, “Artificial neural networks for solving ordinary and partial differential equations”, *IEEE Transactions on Neural Networks*, vol. 9, no. 5, pp. 987–1000, 1998.
- [8] J. Sirignano and K. Spiliopoulos, “DGM: A deep learning algorithm for solving partial differential equations”, *Journal of Computational Physics*, vol. 375, pp. 1339–1364, 2018.
- [9] Y. Liao and P. Ming, “Deep Nitsche Method: Deep Ritz Method with Essential Boundary Conditions”, *Communications in Computational Physics*, vol. 29, no. 5, pp. 1365–1384, 2021.
- [10] G. Pang, L. Lu, and G. E. Karniadakis, “fPINNs: Fractional Physics-Informed Neural Networks”, *SIAM Journal on Scientific Computing*, vol. 41, no. 4, A2603–A2626, 2019.
- [11] Z. Hu, A. D. Jagtap, G. E. Karniadakis, and K. Kawaguchi, “When Do Extended Physics-Informed Neural Networks (XPINNs) Improve Generalization?”, *SIAM Journal on Scientific Computing*, vol. 44, no. 5, A3158–A3182, 2022.
- [12] P. Bochev and M. Gunzburger, *Least-Squares Finite Element Methods*, ser. Applied Mathematical Sciences. Springer New York, 2009, ISBN: 9780387689227.
- [13] R. G. Patel, I. Manickam, N. A. Trask, M. A. Wood, M. Lee, I. Tomas, and E. C. Cyr, “Thermodynamically consistent physics-informed neural networks for hyperbolic systems”, *Journal of Computational Physics*, vol. 449, p. 110 754, 2022, ISSN: 0021-9991.
- [14] P. Minakowski and T. Richter, “A priori and a posteriori error estimates for the Deep Ritz method applied to the Laplace and Stokes problem”, *Journal of Computational and Applied Mathematics*, vol. 421, p. 114 845, 2023.
- [15] Y. Shin, Z. Zhang, and G. E. Karniadakis, “Error estimates of residual minimization using neural networks for linear PDEs”, *arXiv:2010.08019*, Oct. 2020.
- [16] T. De Ryck and S. Mishra, “Generic bounds on the approximation error for physics-informed (and) operator learning”, *arXiv:2205.11393*, 2022.
- [17] T. De Ryck, S. Mishra, and R. Molinaro, “wPINNs: Weak Physics informed neural networks for approximating entropy solutions of hyperbolic conservation laws”, *arXiv:2207.08483*, 2022.
- [18] T. De Ryck, S. Lanthaler, and S. Mishra, “On the approximation of functions by tanh neural networks”, *Neural Networks*, vol. 143, pp. 732–750, 2021, ISSN: 0893-6080.
- [19] S. Mishra and R. Molinaro, “Estimates on the generalization error of physics-informed neural networks for approximating PDEs”, *IMA Journal of Numerical Analysis*, Jan. 2022, drab093, ISSN: 0272-4979.
- [20] J.-L. Guermond, “A Finite Element Technique for Solving First-Order PDEs in  $L^p$ ”, *SIAM Journal on Numerical Analysis*, vol. 42, no. 2, pp. 714–737, 2004.
- [21] J.-L. Guermond and B. Popov, “ $L^1$ -minimization methods for Hamilton–Jacobi equations: the one-dimensional case”, *Numerische Mathematik*, vol. 109, no. 2, pp. 269–284, 2008, ISSN: 0945-3245.
- [22] J.-L. Guermond, F. Marpeau, and B. Popov, “A fast algorithm for solving first-order PDEs by  $L^1$ -minimization”, *Commun. Math. Sci.*, vol. 6, no. 1, pp. 199–216, 2008, ISSN: 1539-6746.
- [23] J. E. Lavery, “Nonoscillatory solution of the steady-state inviscid burgers’ equation by mathematical programming”, *Journal of Computational Physics*, vol. 79, no. 2, pp. 436–448, 1988, ISSN: 0021-9991.
- [24] C. Wang, S. Li, D. He, and L. Wang, “Is  $L^2$  Physics-Informed Loss Always Suitable for Training Physics-Informed Neural Network?”, *arXiv:2206.02016*, 2022.
- [25] E. Kharazmi, Z. Zhang, and G. E. Karniadakis, “Variational Physics-Informed Neural Networks For Solving Partial Differential Equations”, *arXiv:1912.00873*, 2019.
- [26] W. E and B. Yu, “The Deep Ritz Method: A Deep Learning-Based Numerical Algorithm for Solving Variational Problems”, *Communications in Mathematics and Statistics*, vol. 6, no. 1, pp. 1–12, 2018, ISSN: 2194-671X.
- [27] L. Liu, S. Liu, H. Yong, F. Xiong, and T. Yu, “Discontinuity Computing with Physics-Informed Neural Network”, *arXiv:2206.03864*, 2022.
- [28] U. S. Fjordholm, S. Lanthaler, and S. Mishra, “Statistical Solutions of Hyperbolic Conservation Laws: Foundations”, *Archive for Rational Mechanics and Analysis*, vol. 226, no. 2, pp. 809–849, 2017, ISSN: 1432-0673.
- [29] I. Goodfellow, J. Pouget-Abadie, M. Mirza, B. Xu, D. Warde-Farley, S. Ozair, A. Courville, and Y. Bengio, “Generative adversarial networks”, *Communications of the ACM*, vol. 63, no. 11, pp. 139–144, 2020.
- [30] M. Arjovsky, S. Chintala, and L. Bottou, “Wasserstein generative adversarial networks”, in *International conference on machine learning*, PMLR, 2017, pp. 214–223.
- [31] C. Bardos, A. Y. Leroux, and J. C. Nedelec, “First order quasilinear equations with boundary conditions”, *Communications in Partial Differential Equations*, vol. 4, no. 9, pp. 1017–1034, 1979.

- [32] C. I. Kondo and P. G. LeFloch, “Measure-valued solutions and well-posedness of multi-dimensional conservation laws in a bounded domain”, *Port. Math. (N.S.)*, vol. 58, no. 2, pp. 171–193, 2001, issn: 0032-5155.
- [33] C. M. Dafermos, *Hyperbolic conservation laws in continuum physics*, Fourth, ser. Grundlehren der mathematischen Wissenschaften [Fundamental Principles of Mathematical Sciences]. Springer-Verlag, Berlin, 2016, vol. 325.
- [34] E. Y. Panov, “Uniqueness of the solution of the Cauchy problem for a first order quasilinear equation with one admissible strictly convex entropy”, *Mathematical Notes*, vol. 55, no. 5, pp. 517–525, 1994.
- [35] C. De Lellis, F. Otto, and M. Westdickenberg, “Minimal entropy conditions for Burgers equation”, *Quarterly of applied mathematics*, vol. 62, no. 4, pp. 687–700, 2004.
- [36] K. He, X. Zhang, S. Ren, and J. Sun, “Deep Residual Learning for Image Recognition”, in *2016 IEEE Conference on Computer Vision and Pattern Recognition (CVPR)*, 2016, pp. 770–778.
- [37] S. Wang, X. Yu, and P. Perdikaris, “When and why PINNs fail to train: A neural tangent kernel perspective”, *Journal of Computational Physics*, vol. 449, p. 110 768, 2022, issn: 0021-9991.
- [38] J. Chen, “A Comparison Study of Deep Galerkin Method and Deep Ritz Method for Elliptic Problems with Different Boundary Conditions”, *Communications in Mathematical Research*, vol. 36, no. 3, pp. 354–376, 2020.
- [39] S. Wang, Y. Teng, and P. Perdikaris, “Understanding and Mitigating Gradient Flow Pathologies in Physics-Informed Neural Networks”, *SIAM Journal on Scientific Computing*, vol. 43, no. 5, A3055–A3081, 2021.
- [40] D. P. Kingma and J. Ba, “Adam: A Method for Stochastic Optimization”, in *3rd International Conference on Learning Representations, ICLR 2015, San Diego, CA, USA, May 7-9, 2015, Conference Track Proceedings*, Y. Bengio and Y. LeCun, Eds., 2015.
- [41] S. J. Reddi, S. Kale, and S. Kumar, “On the Convergence of Adam and Beyond”, in *6th International Conference on Learning Representations, ICLR 2018, Vancouver, BC, Canada, April 30 - May 3, 2018, Conference Track Proceedings*, 2018.
- [42] L. N. Smith, “Cyclical Learning Rates for Training Neural Networks”, in *2017 IEEE Winter Conference on Applications of Computer Vision (WACV)*, 2017, pp. 464–472.
- [43] D. I. Ketcheson, K. T. Mandli, A. J. Ahmadi, A. Alghamdi, M. Quezada de Luna, M. Parsani, M. G. Knepley, and M. Emmett, “PyClaw: Accessible, Extensible, Scalable Tools for Wave Propagation Problems”, *SIAM Journal on Scientific Computing*, vol. 34, no. 4, pp. C210–C231, Nov. 2012.